Article

MS/MS-guided isolation of clarinoside, a new anti-inflammatory pentalogin derivative

Coralie Audoin [1], Adam Zampalégré [1], Natacha Blanchet [1], Alexandre Giuliani [2,3], Emmanuel Roulland [4], Olivier Laprévote [4,5] and Grégory Genta-Jouve [4,*]

[1] Laboratoires Clarins, 5 rue Ampère, 95300 Pontoise, France;
[2] DISCO Beamline, Synchrotron SOLEIL, 91192, Gif-sur-Yvette, France ;
[3] UAR1008,CEPIA, INRA, 44316 Nantes, France ;
[4] C-TAC, UMR 8638 CNRS, Université Paris Descartes, Sorbonne Paris Cité, Faculté de Parmacie de Paris, 4 avenue de l'Observatoire, 75006 Paris, France;
[5] Department of Biochemistry, Hôpital Européen Georges Pompidou, AH-HP, 75015 Paris, France
* Correspondence: gregory.genta-jouve@parisdescartes.fr; Tel.: +33 173 531 585

Abstract: Re-investigation of the chemical composition of the annual plant *Mitracarpus scaber* Zucc. led to the identification of a new pentalogin derivative containing a rare quinovose moiety. While the planar structure has been fully determined using tandem MS and quantum mechanics calculations (QM), the tridimensional structure was unraveled after isolation and NMR analysis. The absolute configuration was assigned by comparison of experimental and theoretical SRCD spectra. Both compounds were tested for anti-inflammatory activity and compound **1** showed the ability to inhibit the production of interleukin-8 (Il-8) with an IC_{50} of 9.17 μM

Keywords: *Mitracarpus scaber* Zucc.; pentalogin; anti-inflammatory; MS/MS; Il-8

1. Introduction

Mass spectrometry has become a very convenient technique for the targeted search of new bioactive metabolites[1,2] and the recent introduction of the Global Natural Product Social molecular networking (GNPS) Web-platform (http://gnps.ucsd.edu) enabled the quick and automatic spectral mining of MS/MS spectra[3]. In our ongoing research for bioactive compounds, we decided to re-investigate the chemical composition of *Mitracarpus scaber* Zucc. using a MS/MS-guided approach. *M. scaber* is an annual plant used in African traditional medicine endowed with antifungal, antimicrobial and anti-inflammatory properties [4,5]. Indeed in West Africa the leaves of *M. scaber* are widely used for headache, toothache, amenorrhoea, dyspepsia, hepatic diseases, venereal diseases, leprosy and for the treatment of skin diseases such as scabies, infectious dermatitis and eczema. It is well known to contain phenols[5], flavonoid glycosides[5], furanocoumarines[5], terpenes[6], alkaloids[7] and pentalongin derivatives[8,9]. Herein we report the identification of clarinoside (**1**), a new pentalongin derivative exhibiting the rare quinovose moiety along with the known harounoside (**2**). Both compounds have been tested for anti-inflammatory activity by evaluating their ability to inhibit the production of interleukin-8 (Il-8).

Preprints (www.preprints.org) | NOT PEER-REVIEWED | Posted: 26 March 2018 doi:10.20944/preprints201803.0209.v1

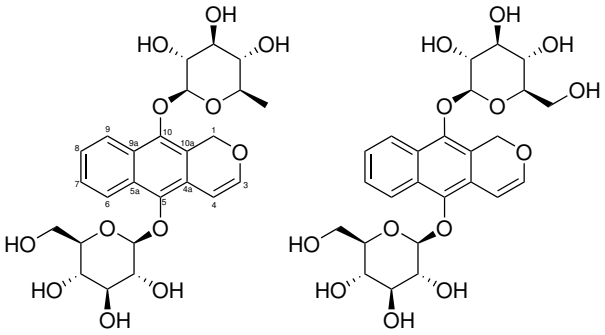

2. Results

The analysis started by the creation of a molecular network of the ethanolic extract of *M. scaber*. The data dependent analysis (DDA) LC-MS/MS data have been uploaded to the GNPS platform and a network has been generated using the parameters listed in the materials and method section below (Figure 1). As an anchor (reference) compound, harounoside (**2**) was used. Its node was quickly "illuminated" using the high resolution MS data and the fragmentation pattern. The *m*/*z* at 561.159 corresponding to the $[M+Na]^+$ adduct of **2** was identified while the two diagnostic fragments were well identified on the MS/MS spectrum (see supporting information), a first one resulting from the cleavage of one O–C bond between the aglycone and a glucose moiety at *m*/*z* 399.1080 $[M\text{-}Glc+Na]^+$ and a second one at *m*/*z* 236.0452 resulting from the cleavage of the second O–C between the aglycone and the other glucose $[M\text{-}2Glc+Na]^{\bullet+}$. In order to seek for the structurally related compounds, the cluster was further studied by annotating the edges with *m*/*z* differences corresponding to known (bio)chemical modifications implemented in the MetaNetter 2 package [10]. Out of the 307 nodes of the network, one node directly connected to harounoside (**2**) with a *m*/*z* difference of -15.995 attracted our attention. According to the biotransformation list available in the MetaNetter package, this difference corresponded to a dehydroxylation.

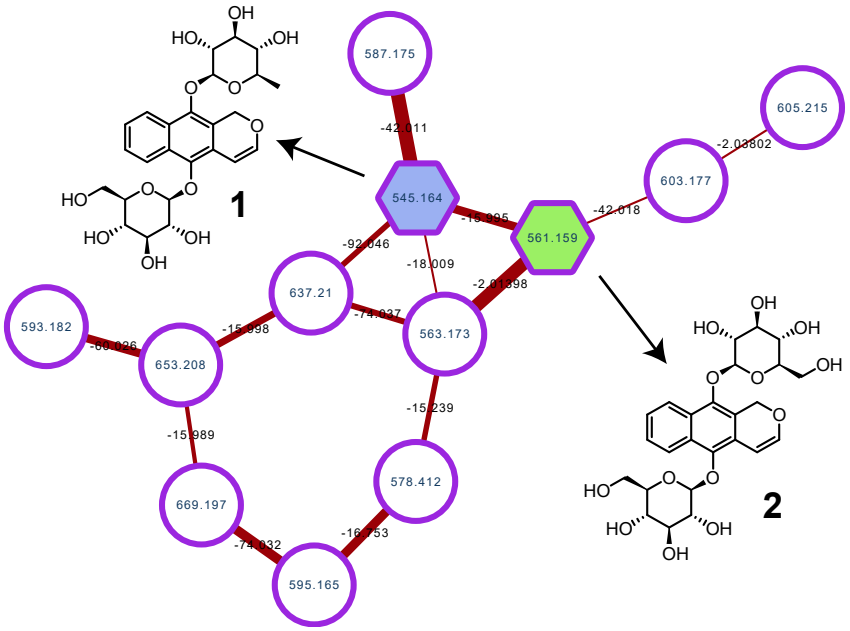

Figure 1. selected cluster containing clarinoside (**1**) and harounoside (**2**)

Considering the structure of **2**, the dehydroxylation could occur at several positions of each of the two sugars. In order to know on which side of the compound **2** the deshydroxylation site was located,

Preprints (www.preprints.org) | NOT PEER-REVIEWED | Posted: 26 March 2018 doi:10.20944/preprints201803.0209.v1

the fragmentation of both glucose moieties was studied using quantum mechanic (QM). The energy profile of the homolytic dissociation was predicted using the B3LYP method at the STO-3G level (See supporting information). The calculations predicted a difference of ca. +2.5 eV in favor of the C5–O–C indicating that the first fragment observed at m/z 399.1080 was related to the loss of one glucose at C-10. This energy difference was very supportive and based on these theoretical results, an energy resolved mass spectrometry (ERMS) study [11] was undertaken in order to determine the stability of the two C–O–C bonds (C5–O–C or C10–O–C) of compound **1**. After selection of the parent ion at m/z 545.1685, the intensity of the ion at 399.1080 was recorded using an increasing value of collision energy (CID). After the complete extinction of the parent ion, the daughter ion at m/z 399.1080 was then fragmented into the one major ion at m/z 185.0433 using the same approach. As shown on figure 2, the C–O–C bond linking the aglycone to the dehydroxyglucose moiety is weaker than the second one as it requires a lower CE value for a 50% dissociation (ca. 15 and 17 for C10–O–C and C5–O–C respectively).

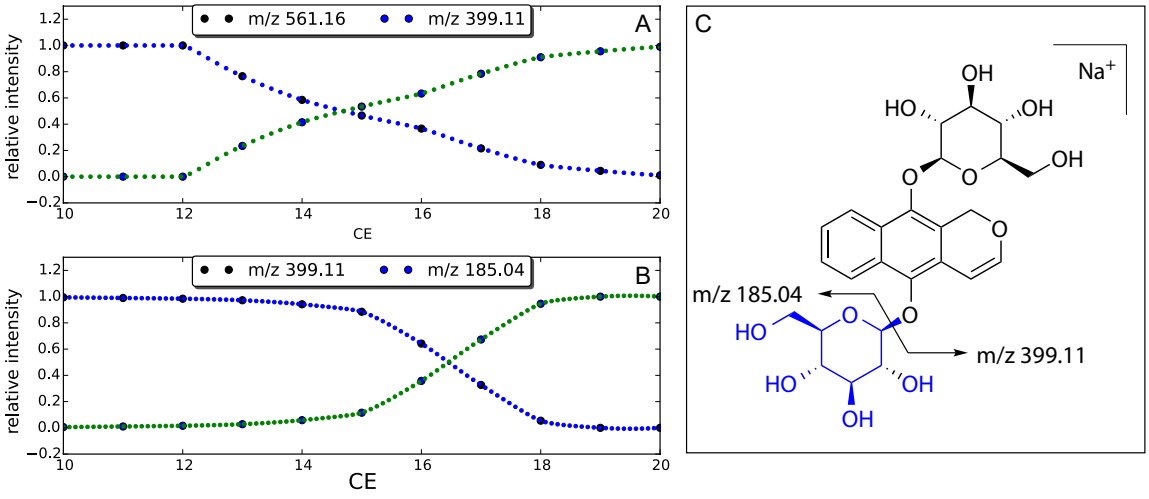

Figure 2. Plot of relative ion current versus collision energy corresponding to m/z 561.16 vs 399.10 (**A**) and m/z 399.10 vs 185.04 (**B**); **C**: MS/MS Fragments of **2**.

The structural elucidation of **1** was pursued with the identification of the neutral loss of 146.0605 Da resulting from the difference between the cationized molecule 545.1685 $[M+Na]^+$ and the fragment at m/z 399.1080. In parallel with the loss of 162.05 Da corresponding to the 2-hydroxymethyl-3,4-dihydro-2*H*-pyran-3,4,5-triol observed for compound **2**, the loss of 146.0605 was consistent with a 2-methyl-3,4-dihydro-2*H*-pyran-3,4,5-triol originating from a deoxyhexose such as fucose, rhamnose or quinovose. Unfortunately, and despite the use of a recent methodology to distinguish the mono-saccharides using MS/MS[12], it was not possible to determine the relative stereo-chemistry of the sugar moieties using MS analysis only, so the isolation of compound **1** was undertaken.

After a reverse phase HPLC purification, 84 mg of compound **1** was obtained and a full set of NMR experiments was performed. The structure of the aglycone was confirmed by comparison of the ^{1}H and ^{13}C NMR chemical shifts (see table 1). The nature of the sugar was determined by taking advantage of the newly published methodology by Giner *et al.*[13] which is based on a acid-promoted hydrolysis of the studied compound performed directly in the deuterated NMR solvent. Looking at the ^{1}H NMR spectrum, the doublets at δ 4.66 (J = 7.7 Hz) and 4.79 (J = 7.8 Hz) ppm clearly confirmed a glucose and a quinovose moieties (see supporting information). According to the ERMS data, the quinovose was located at C-10 and this was confirmed by the two ^3J coupling between H-1′/C-10 and H-1"/C-5 on the HMBC spectrum. The detailed NMR data are given in the table 1.

Preprints (www.preprints.org) | NOT PEER-REVIEWED | Posted: 26 March 2018 doi:10.20944/preprints201803.0209.v1

Table 1. ^{1}H and ^{13}C NMR data for **1** at 600 MHz in CD_3OD (δ_H in ppm)

no.	δ_H (multiplicity, *J*)	δ_C	no.	δ_H (multiplicity, *J*)	δ_C
1	5.29 (dd, 40.7, 13.8 Hz)	65.2	1′	4.66 (d, 7.8)	106.2
3	6.67 (dd, 14.4, 5.9 Hz)	147.8	2′	3.61 (dd, 9.0, 7.8)	75.9
4	6.66 (dd 14.4, 5.9 Hz)	102.1	3′	3.38 (t, 9.0)	77.7
4a		121.6	4′	3.11 (t, 9.0)	73.5
5		143.3	5′	3.11 (m)	77.8
5a		131.0	6′	1.21 (d, 5.4)	18.1
6	8.43 (d, 8.2 Hz)	124.7	1"	4.79 (d, 7.8)	106.9
7	7.44 (dt, 8.2, 1 Hz)	127.0	2"	3.65 (m)	75.8
8	7.40 (dt, 8.2, 1 Hz)	126.2	3"	3.46 (m)	71.5
9	8.41 (d, 8.2 Hz)	123.7	4"	3.14 (m)	76.9
9a		129.1	5"	3.47 (t, 9.0)	78.0
10		144.9	6"	3.67 (m)	62.7
10a		122.6			

The absolute configuration of compound **1** was determined by comparison of an synchrotron radiation circular dichroism (SRCD) spectrum with theoretical electronic circular dichroism (ECD) spectrum (figure 3). Unexpectedly, the ECD spectrum was quite complex with four Cotton effect (CE) was of alternative signs. The calculation have been run on the four diasteroisomers, ie. *D*-Glc/*D*-Qui, *D*-Glc/*L*-Qui, *L*-Glc/*D*-Qui and *L*-Glc/*L*-Qui. While the absolute *D* configuration of the glucose moiety was expected, as it is well known that higher plants produce only this enantiomer [14], the absolute configuration of the quinovose moiety was not trivial because the quinovose can originate from both *D*-glucose [15] or *L*-fucose [16]. A very good agreement was only observed between one

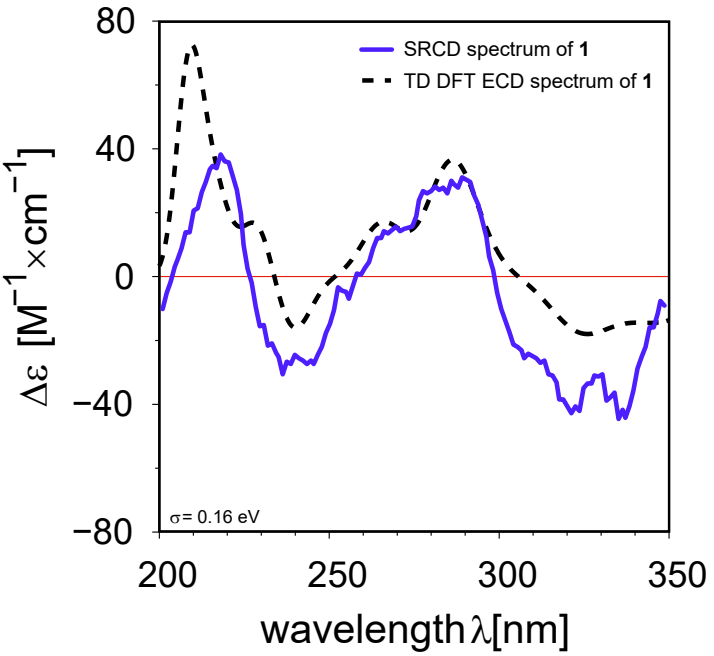

Figure 3. Overlay of SRCD and TD DFT spectra of **1**

theoretical (*D*-Glc/*D*-Qui) and the experimental spectra so that the compound **1** could be named 5,10-dihydroxy-2*H*-naphtho[2,3-b]-pyran-5-*β*-*D*-glucopyranosyl-10-*β*-*D*-quinovopyranoside.

Both compounds **1** and **2** were tested for anti-inflammatory activity by measuring their ability to inhibit the production of interleukin-8 (Il-8), one of the key mediator associated with

Preprints (www.preprints.org) | NOT PEER-REVIEWED | Posted: 26 March 2018 doi:10.20944/preprints201803.0209.v1

inflammation[17,18]. After exposure to the tumor necrosis factor alpha (TNFα) at 0.5 ng mL^{-1} for 24 hours, the production of Il-8 was measured and compared to the known anti-inflammatory standard epigallocatechin gallate (EGCG). As shown in figure 4, the TNFα is inducing the production of Il-8 of 398.37$\pm$24.09 pg/mg of total protein while the addition of EGCG at 21.8 μM allows a return to the basal threshold of 33.01$\pm$2.12 pg/mg of total protein. Although the two compounds were tested during two independent tests, the differences in the measured concentrations (ie. the production of Il-8 and its inhibition) were observed in both experiments. A nice correlation (R^2=0.996) is observed

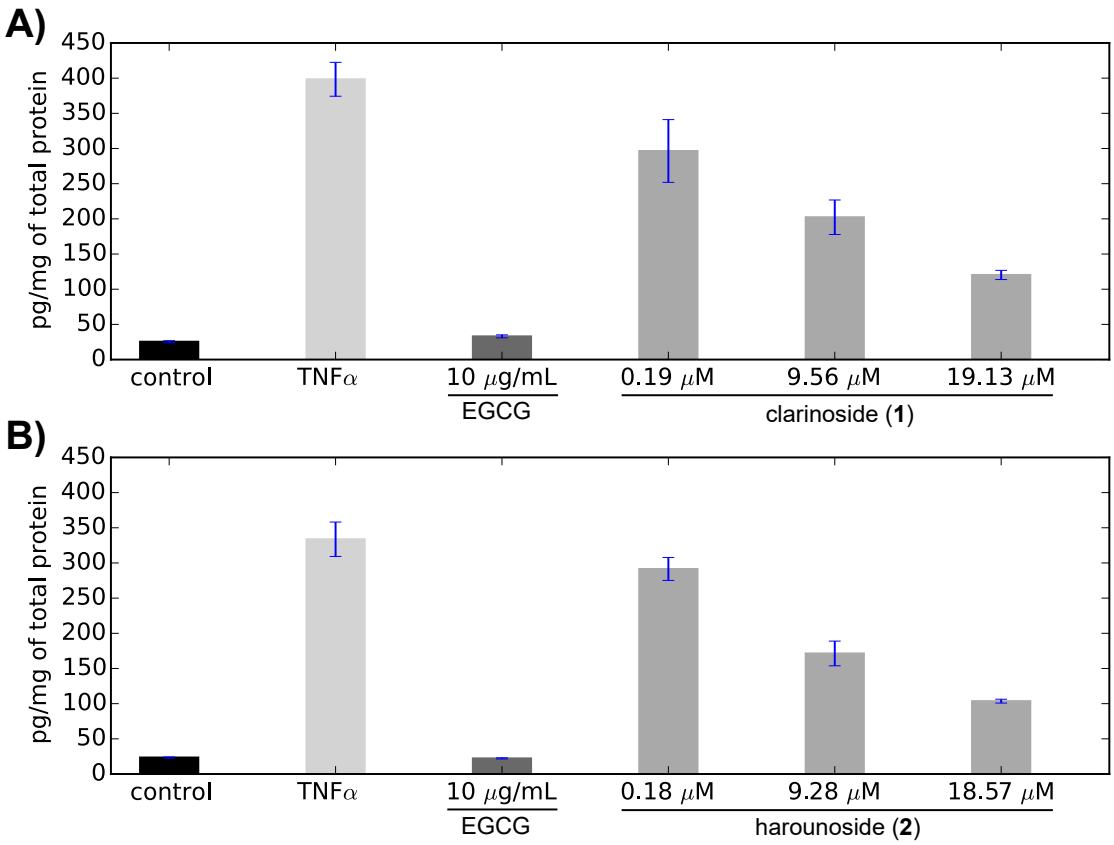

Figure 4. Inhibition of the interleukin-8 (Il-8) production: **A** clarinoside (**1**) ; **B** harounoside **(2)**

between the inhibition of the production of Il-8 and the concentration of clarinoside (**1**). A IC_{50} of 9.17 μM has been measured while a total inhibition of the Il-8 production at 36 μM can be extrapolated. The IC_{50} of **1** is of the same order of magnitude as that of EGCG (10.9 μM[19]), although slightly lower. Interestingly, the IC_{50} of **2** (9.21 μM), is very similar to the one measured for compound **1**, indicating that the structural modification has no impact on its biological activity.

To conclude, this study enabled the rapid identification of one new compound from *M. scaber*. The biological activity evaluation highlighted the ability of compounds **1** and **2** to inhibit the production of Il-8 confirming the importance of *M. scaber* metabolites and their possible use in comestics.

3. Materials and Methods

General procedure

The preparative HPLC was performed on a VWR LaPrep P110 system using a C-630 Büchi UV detector. NMR spectra acquisition has been realized using a 600 MHz Bruker Avance spectrometer equipped with Z-gradients and a triple resonance TXI probe. The signals were referenced in ppm to the residual solvent signals (CD_3OD, at δ_H 3.31 and δ_C 49.0). The infra-red spectrum has been acquired

Preprints (www.preprints.org) | NOT PEER-REVIEWED | Posted: 26 March 2018 doi:10.20944/preprints201803.0209.v1

on a Nicolet IS50 FT-IR spectrophotometer. The specific rotation has been measured using a Anton Paar MCP150 polarimeter.

Plant material

The flowered aerial parts of *Mitracarpus Scaber* were collected in Burkina Faso in the town of Poun and then dried in the same area.

Extraction and purification

An ethanolic extraction was performed on a 300 g sample of dried plant with a ratio plant/solvent of 1/7 yealding 16.5 g of crude extract which was then directly processed by reverse phase with an XBridge Prep C18, 5 μm (OBD 30 $\times$ 250 mm) preparative HPLC column. A gradient H_2O/MeOH (starting from 90:10 to 70/30 in 30 minutes at 100 mL min^{-1}) was used to afford the compounds **1** (84 mg) and **2** (113 mg).

LC-MS data acquisition and processing

A XEVO-G2 XS QTOF (Waters) equipped with an electrospray ionization (ESI) source was used for the qualitative analysis of the extract. A first screening analysis was performed using the MS^E technology (Waters) on a mass range from 50 to 1500 Da. The optimal ionization source working parameters were as follows: capillary voltage, 3.0 kV; sampling cone, 40 V; extraction cone, 6.0 V; source temperature, 150 °C; desolvation temperature, 600 °C; cone gas flow, 50 L/h; desolvation gas flow, 1000 L/h. MS/MS data was obtained using a data dependent analysis (DDA) with the same ionization parameters as above using three different collision energies: 10, 20 and 40 V.

Construction of the molecular network

A molecular network was created using the online workflow at GNPS[3]. The data was filtered by removing all MS/MS peaks within +/- 17 Da of the precursor m/z. MS/MS spectra were window filtered by choosing only the top 6 peaks in the +/- 50 Da window throughout the spectrum. The data was then clustered with MS-Cluster with a parent mass tolerance of 2.0 Da and a MS/MS fragment ion tolerance of 0.5 Da to create consensus spectra . Further, consensus spectra that contained less than 2 spectra were discarded. A network was then created where edges were filtered to have a cosine score above 0.7 and more than 3 matched peaks. Further edges between two nodes were kept in the network if and only if each of the nodes appeared in each other's respective top 10 most similar nodes. The spectra in the network were then searched against GNPS' spectral libraries. The library spectra were filtered in the same manner as the input data. All matches kept between network spectra and library spectra were required to have a score above 0.7 and at least 6 matched peaks.

Energy resolved mass spectrometry

The LTQ-Orbitrap XL mass spectrometer (Thermo Scientific (Bremen), Bremen, Germany) was used for the ERMS study. The analysis was performed in positive ion mode with a mass range of m/z 100–1100. The optimized ESI parameters were set as follows: capillary temperature of 250 °C; sheath gas (nitrogen) flow of 30 arb.; auxiliary gas (nitrogen) flow of 10 arb.; source voltage of 4.25 kV; capillary voltage of 25 V; tube lens voltage of 110 V. The resolution of the orbitrap mass analyzer was set at 30,000. The isolation width was 2 amu, and the normalized collision energy (CE) was set from 10 to 20. Collision-induced dissociation (CID) was conducted in LTQ with an activation q of 0.25 and activation time of 30 ms. All instruments were controlled by the Xcalibur data system, and the data acquisition was carried out by analyst software Xcalibur (version 2.1) (Waltham, MA, USA) from Thermo Electron Corp.

 doi:10.20944/preprints201803.0209.v1

Synchrotron Radiation Circular Dichroism

The SRCD experiments have been carried out on the SRCD station [20] DISCO beamline [21] at the SOLEIL synchrotron (Gif-sur-Yvette, France). The sample were placed in calcium fluoride cells of 100 microns optical path length and measured at 0.2 mol/l in methanol. (+)-camphor-10-sulfonic acid (CSA) solution was used to calibrate the SRCD signal. For each sample three spectra were collected in the 350 - 200 nm range with 1 nm step and 1200 ms integration time. The molar circular dichroism $\Delta\epsilon$ is expressed in M^{-1} cm^{-1}.

Computational details

All QM calculations were carried out using Gaussian 16[22]. The energy scan of the C–O bonds was performed using the Hartree-Fock method at the STO-3G level and a 0.1 Å bond length step.The GMMX package was used for the conformational analysis (force field: MMFF94). The TD DFT calculations have been performed using the B3LYP method at the 6-31G(d) level for 20 excited states. The SpecDis 1.71 software was used to plot the ECD spectrum[23].

Cell culture

HaCaT Keratinocytes cells were cultured under standard conditions in DMEM medium supplemented with 10% fetal calf serum. The medium was changed every second day. Confluent cultures were removed by trypsin incubation, and then the cells were counted. They were seeded into 96-well culture microplates at a density of 30,000 cells per well (200 μ L) and kept at 37 °C for 24 h.

Interleukine release measurement

The release of IL-8 in cell supernatants was determined by ELISA. After TNF-α incubation (0.5 ng/mL), cell supernatants were harvested and stored at -20 °C until use for measurements. The quantity of released Il-8 was measured according to the manufacturer's instructions (Kit ELISA Human CXCL8 / IL8 R&D Systems). The decease in Il-8 production by EGCG (10 μg/mL) validated the method.

Compound Characterization

1: White, amorphous solid; $[\alpha]_D^{20}$ + (c 0.25, CH_3OH); UV (DAD) λ_{max} 223, 245, 284, 346 nm; ^1H NMR and ^{13}C NMR data see Table 1; HRESIMS (+) m/z 545.1685 $[M + Na]^+$ (545,16295 calcd. for $C_{25}H_{30}O12Na$, Δ -1.8 ppm).

Supplementary Materials: Supplementary materials, including, HRMS, 1D and 2D NMR spectra for compound **1**, and computational details for **1**, are available on-line.

Acknowledgments: SOLEIL support is acknowledged under proposal number 20170521. We also thank the technical staff of SOLEIL for smooth and efficient running of the facility. The authors are grateful to Pascale Leproux and Karim Hammad for MS and NMR spectra recording.

Author Contributions: G.G.J. and C.A. conceived and designed the experiments; C.A., A.Z., N.B., E.R. and G.G.J. performed the experiments; C.A., O.L. and G.G.J analyzed the data; A.G. and E.R. contributed reagents/materials/analysis tools; All the authors wrote the paper.

Conflicts of Interest: The authors declare no conflict of interest.

References

1. Olivon, F.; Allard, P.M.; Koval, A.; Righi, D.; Genta-Jouve, G.; Neyts, J.; Apel, C.; Pannecouque, C.; Nothias, L.F.; Cachet, X.; Marcourt, L.; Roussi, F.; Katanaev, V.L.; Touboul, D.; Wolfender, J.L.; Litaudon, M. Bioactive Natural Products Prioritization Using Massive Multi-informational Molecular Networks. *ACS Chemical Biology* **2017**, *12*, 2644–2651. PMID: 28829118.
2. Nothias, L.F.; Nothias-Esposito, M.; da Silva, R.; Wang, M.; Protsyuk, I.; Zhang, Z.; Sarvepalli, A.; Leyssen, P.; Touboul, D.; Costa, J.; Paolini, J.; Alexandrov, T.; Litaudon, M.; Dorrestein, P.C. Bioactivity-Based

Molecular Networking for the Discovery of Drug Leads in Natural Product Bioassay-Guided Fractionation. *Journal of Natural Products* **0**, *0*, null.

3. Wang, M.; Carver, J.J.; Phelan, V.V.; Sanchez, L.M.; Garg, N.; Peng, Y.; Nguyen, D.D.; Watrous, J.; Kapono, C.A.; Luzzatto-Knaan, T.; Porto, C.; Bouslimani, A.; Melnik, A.V.; Meehan, M.J.; Liu, W.T.; Crüsemann, M.; Boudreau, P.D.; Esquenazi, E.; Sandoval-Calderón, M.; Kersten, R.D.; Pace, L.A.; Quinn, R.A.; Duncan, K.R.; Hsu, C.C.; Floros, D.J.; Gavilan, R.G.; Kleigrewe, K.; Northen, T.; Dutton, R.J.; Parrot, D.; Carlson, E.E.; Aigle, B.; Michelsen, C.F.; Jelsbak, L.; Sohlenkamp, C.; Pevzner, P.; Edlund, A.; McLean, J.; Piel, J.; Murphy, B.T.; Gerwick, L.; Liaw, C.C.; Yang, Y.L.; Humpf, H.U.; Maansson, M.; Keyzers, R.A.; Sims, A.C.; Johnson, A.R.; Sidebottom, A.M.; Sedio, B.E.; Klitgaard, A.; Larson, C.B.; Boya P, C.A.; Torres-Mendoza, D.; Gonzalez, D.J.; Silva, D.B.; Marques, L.M.; Demarque, D.P.; Pociute, E.; O'Neill, E.C.; Briand, E.; Helfrich, E.J.N.; Granatosky, E.A.; Glukhov, E.; Ryffel, F.; Houson, H.; Mohimani, H.; Kharbush, J.J.; Zeng, Y.; Vorholt, J.A.; Kurita, K.L.; Charusanti, P.; McPhail, K.L.; Nielsen, K.F.; Vuong, L.; Elfeki, M.; Traxler, M.F.; Engene, N.; Koyama, N.; Vining, O.B.; Baric, R.; Silva, R.R.; Mascuch, S.J.; Tomasi, S.; Jenkins, S.; Macherla, V.; Hoffman, T.; Agarwal, V.; Williams, P.G.; Dai, J.; Neupane, R.; Gurr, J.; Rodríguez, A.M.C.; Lamsa, A.; Zhang, C.; Dorrestein, K.; Duggan, B.M.; Almaliti, J.; Allard, P.M.; Phapale, P.; Nothias, L.F.; Alexandrov, T.; Litaudon, M.; Wolfender, J.L.; Kyle, J.E.; Metz, T.O.; Peryea, T.; Nguyen, D.T.; VanLeer, D.; Shinn, P.; Jadhav, A.; Müller, R.; Waters, K.M.; Shi, W.; Liu, X.; Zhang, L.; Knight, R.; Jensen, P.R.; Palsson, B.Ø.; Pogliano, K.; Linington, R.G.; Gutiérrez, M.; Lopes, N.P.; Gerwick, W.H.; Moore, B.S.; Dorrestein, P.C.; Bandeira, N. Sharing and community curation of mass spectrometry data with Global Natural Products Social Molecular Networking. *Nature Biotechnology* **2016**, *34*, 828 EP –.
4. Ekpendu, T.O.; Akah, P.A.; Adesomoju, A.A.; Okogun, J.I. Antiinflammatory and Antimicrobial Activities of *Mitracarpus scaber* Extracts. *International Journal of Pharmacognosy* **1994**, *32*, 191–196.
5. Bisignano, G.; Sanogo, R.; Marino, A.; Aquino, R.; 'angelo, V.D.; Germano, M.P.; De Pasquale, R.; Pizza, C. Antimicrobial activity of *Mitracarpus scaber* extract and isolated constituents. *Letters in Applied Microbiology* **2000**, *30*, 105–108.
6. Gbaguidi, F.; Accrombessi, G.; Moudachirou, M.; Quetin-Leclercq, J. HPLC quantification of two isomeric triterpenic acids isolated from Mitracarpus scaber and antimicrobial activity on Dermatophilus congolensis. *Journal of Pharmaceutical and Biomedical Analysis* **2005**, *39*, 990 – 995.
7. Okunade, A.L.; Clark, A.M.; Hufford, C.D.; Oguntimein, B.O. Azaanthraquinone: An Antimicrobial Alkaloid from *Mitracarpus scaber*. *Planta Medica* **1999**, *65*, 447–448.
8. Harouna, H.; Faure, R.; Elias, R.; Debrauwer, L.; Saadou, M.; Balansard, G.; Boudon, G. Harounoside a pentalongin hydroquinone diglycoside from Mitracarpus scaber. *Phytochemistry* **1995**, *39*, 1483 – 1484.
9. Pialat, J.P.; Hoffmann, P.; Moulis, C.; Fouraste, I.; Labidalle, S. Synthesis and Extraction of Pentalongin, A Naphthoquinoid From Mitracarpus Scaber. *Natural Product Letters* **1998**, *12*, 23–30.
10. Burgess, K.; Borutzki, Y.; Rankin, N.; Daly, R.; Jourdan, F. MetaNetter 2: A Cytoscape plugin for ab initio network analysis and metabolite feature classification. *Journal of Chromatography B* **2017**.
11. Menachery, S.P.M.; Laprévote, O.; Nguyen, T.P.; Aravind, U.K.; Gopinathan, P.; Aravindakumar, C.T. Identification of position isomers by energy-resolved mass spectrometry. *Journal of Mass Spectrometry* **2015**, *50*, 944–950.
12. Xia, B.; Zhou, Y.; Liu, X.; Xiao, J.; Liu, Q.; Gu, Y.; Ding, L. Use of electrospray ionization ion-trap tandem mass spectrometry and principal component analysis to directly distinguish monosaccharides. *Rapid Communications in Mass Spectrometry* **2012**, *26*, 1259–1264.
13. Giner, J.L.; Feng, J.; Kiemle, D.J. NMR Tube Degradation Method for Sugar Analysis of Glycosides. *Journal of Natural Products* **2016**, *79*, 2413–2417. PMID: 27603739.
14. Genta-Jouve, G.; Weinberg, L.; Cocandeau, V.; Maestro, Y.; Thomas, O.P.; Holderith, S. Revising the Absolute Configurations of Coatlines via Density Functional Theory Calculations of Electronic Circular Dichroism Spectra. *Chirality* **2013**, *25*, 180–184.
15. Han, A.R.; Park, S.R.; Park, J.W.; Lee, E.Y.; Kim, D.M.; Kim, B.G.; Yoon, Y.J. Biosynthesis of Glycosylated Derivatives of Tylosin in Streptomyces venezuelae. *J. Microbiol. Biotechnol* **2011**, *21*, 613–616.
16. De Castro, C.; Kenyon, J.J.; Cunneen, M.M.; Molinaro, A.; Holst, O.; Skurnik, M.; Reeves, P.R. The O-specific polysaccharide structure and gene cluster of serotype O:12 of the *Yersinia pseudotuberculosis* complex, and the identification of a novel l-quinovose biosynthesis gene. *Glycobiology* **2013**, *23*, 346–353.

17. Baggiolini, M.; Clark-Lewis, I. Interleukin-8, a chemotactic and inflammatory cytokine. *FEBS Letters* **1992**, *307*, 97–101.
18. Pease, J.E.; Sabroe, I. The Role of Interleukin-8 and its Receptors in Inflammatory Lung Disease. *American Journal of Respiratory Medicine* **2002**, *1*, 19–25.
19. of EGCG has been measured on a previous experiment., T.I.
20. Réfrégiers, M.; Wien, F.; Ta, H.P.; Premvardhan, L.; Bac, S.; Jamme, F.; Rouam, V.; Lagarde, B.; Polack, F.; Giorgetta, J.L.; Ricaud, J.P.; Bordessoule, M.; Giuliani, A. DISCO synchrotron-radiation circular-dichroism endstation at SOLEIL. *Journal of Synchrotron Radiation* **2012**, *19*, 831–835.
21. Giuliani, A.; Jamme, F.; Rouam, V.; Wien, F.; Giorgetta, J.L.; Lagarde, B.; Chubar, O.; Bac, S.; Yao, I.; Rey, S.; Herbeaux, C.; Marlats, J.L.; Zerbib, D.; Polack, F.; Réfrégiers, M. DISCO: A low-energy multipurpose beamline at synchrotron SOLEIL. *Journal of Synchrotron Radiation* **2009**, *16*, 835–841.
22. Frisch, M.J.; Trucks, G.W.; Schlegel, H.B.; Scuseria, G.E.; Robb, M.A.; Cheeseman, J.R.; Scalmani, G.; Barone, V.; Petersson, G.A.; Nakatsuji, H.; Li, X.; Caricato, M.; Marenich, A.V.; Bloino, J.; Janesko, B.G.; Gomperts, R.; Mennucci, B.; Hratchian, H.P.; Ortiz, J.V.; Izmaylov, A.F.; Sonnenberg, J.L.; Williams-Young, D.; Ding, F.; Lipparini, F.; Egidi, F.; Goings, J.; Peng, B.; Petrone, A.; Henderson, T.; Ranasinghe, D.; Zakrzewski, V.G.; Gao, J.; Rega, N.; Zheng, G.; Liang, W.; Hada, M.; Ehara, M.; Toyota, K.; Fukuda, R.; Hasegawa, J.; Ishida, M.; Nakajima, T.; Honda, Y.; Kitao, O.; Nakai, H.; Vreven, T.; Throssell, K.; Montgomery, Jr., J.A.; Peralta, J.E.; Ogliaro, F.; Bearpark, M.J.; Heyd, J.J.; Brothers, E.N.; Kudin, K.N.; Staroverov, V.N.; Keith, T.A.; Kobayashi, R.; Normand, J.; Raghavachari, K.; Rendell, A.P.; Burant, J.C.; Iyengar, S.S.; Tomasi, J.; Cossi, M.; Millam, J.M.; Klene, M.; Adamo, C.; Cammi, R.; Ochterski, J.W.; Martin, R.L.; Morokuma, K.; Farkas, O.; Foresman, J.B.; Fox, D.J. Gaussian~16 Revision B.01, 2016. Gaussian Inc. Wallingford CT.
23. Bruhn, T.; Schaumlöffel, A.; Hemberger, Y.; Bringmann, G. SpecDis: Quantifying the Comparison of Calculated and Experimental Electronic Circular Dichroism Spectra. *Chirality* **2013**, *25*, 243–249.

Sample Availability: Samples of the compounds **1** and **2** are available from the authors.